



1 **Current status of model predictions on volatile organic compounds and impacts**
2 **on surface ozone predictions during summer in China**

3 Yongliang She¹, Jingyi Li¹, Xiaopu Lyu², Hai Guo³, Momei Qin¹, Xiaodong Xie¹, Kangjia
4 Gong¹, Fei Ye¹, Jianjiong Mao¹, Lin Huang¹, Jianlin Hu^{1*}

5

6 ¹ *Jiangsu Key Laboratory of Atmospheric Environment Monitoring and Pollution*
7 *Control, Jiangsu Collaborative Innovation Center of Atmospheric Environment and*
8 *Equipment Technology, School of Environmental Science and Engineering, Nanjing*
9 *University of Information Science & Technology, 219 Ningliu Road, Nanjing 210044,*
10 *China*

11 ² *Department of Geography, Hong Kong Baptist University, Hong Kong 000000, China*

12 ³ *Department of Civil and Environmental Engineering, The Hong Kong Polytechnic*
13 *University, Hong Kong 00000, China*

14

15 * Corresponding author:

16 Jianlin Hu, Email: jianlinhu@nuist.edu.cn.



17 **Abstract**

18 Volatile organic compounds (VOCs) play a crucial role in the formation of
19 tropospheric ozone (O₃) and secondary organic aerosols. VOC emissions are generally
20 considered to have larger uncertainties compared to other pollutants, such as sulphur
21 dioxide and fine particulate matter (PM_{2.5}). Although predictions of O₃ and PM_{2.5} have
22 been extensively evaluated in air quality modelling studies, there has been limited
23 reporting on the evaluation of VOCs, mainly due to a lack of routine VOCs
24 measurements at multiple sites. In this study, we utilized VOCs measurements from the
25 ATMSYC project at 28 sites across China and assessed the predicted VOCs
26 concentrations using the Community Multiscale Air Quality (CMAQ) model with the
27 widely used Multi-resolution Emission Inventory for China (MEIC). The ratio of
28 predicted to observed total VOCs was found to be 0.74 ± 0.40 , with underpredictions
29 ranging from 2.05 to 50.61 ppbv (5.77% to 85.40%) at 24 sites. A greater bias in VOCs
30 predictions was observed in industrial cities in the north and southwest, such as Jinan,
31 Shijiazhuang, Lanzhou, Chengdu, and Guiyang. In terms of different VOC components,
32 alkanes, alkenes, non-naphthalene aromatics (ARO2MN), and alkynes were
33 consistently underpredicted, with ratios of predicted to observed of 0.53 ± 0.38 , $0.51 \pm$
34 0.48 , 0.31 ± 0.38 , and 0.41 ± 0.47 , respectively. Sensitivity experiments were conducted
35 to assess the impact of the VOCs prediction bias on O₃ predictions. While emission
36 adjustments improved the model performance for VOCs, resulting in a ratio of total
37 VOCs to 0.86 ± 0.47 , they also exacerbated O₃ overprediction relative to the base case
38 by 0.62% to 6.27% across the sites. This study demonstrates that current modelling
39 setups and emission inventories are likely to underpredict VOCs concentrations, and
40 this underprediction of VOCs contributes to lower O₃ predictions in China.

41 **Keywords:** *volatile organic compounds, O₃ prediction, model evaluation, emissions*



42 **1. Introduction**

43 Volatile organic compounds (VOCs) in the ambient atmosphere consist of
44 thousands of gaseous organic trace substances emitted from various anthropogenic and
45 biogenic sources (Guenther et al., 2012; Li et al., 2017a; Kelly et al., 2018). These
46 compounds undergo complex chemical reactions that form ozone (O₃) and secondary
47 organic aerosols (SOA) (Sillman, 1999; Kroll and Seinfeld, 2008). While biogenic
48 VOCs (BVOCs) are the primary source of VOCs worldwide (Guenther et al., 2006),
49 urban areas are predominantly influenced by anthropogenic sources (Guan et al., 2020;
50 Guo et al., 2022; Li et al., 2022a). Anthropogenic VOCs (AVOCs) emission inventories
51 are typically developed by estimating the total VOCs emissions using emission factors
52 (EFs) and activity rates from different sources. The VOCs speciation profiles are then
53 utilized to determine the emission rates of various VOCs species (Li et al., 2017a). Due
54 to the complexity of VOCs emission processes and presence of numerous small but
55 dispersed nonpoint sources, notable uncertainties exist while determining EFs, activity
56 rates, and speciation profiles. It is estimated that the uncertainties associated with VOCs
57 emissions range from approximately 68% to 76%, which are higher than those of
58 sulphur dioxide (SO₂) (12% to 40%), nitrogen dioxide (NO_x) (31% to 35%), and
59 particulate matter (PM) (30% to 94%) (Zhang et al., 2009; Li et al., 2019; Kurokawa
60 and Ohara, 2020; An et al., 2021).

61 Chemical transport models (CTMs), such as the Community Multiscale Air
62 Quality (CMAQ) model, Weather Research and Forecasting model coupled with
63 Chemistry (WRF-Chem), and Goddard Earth Observing System Chemical transport
64 model (GEOS-Chem) have been developed and widely used to investigate the
65 formation processes, source apportionment, and emission control strategies for various
66 air pollution issues (Zhang et al., 2021; Dang et al., 2021; Wang et al., 2021). The



67 emissions of VOCs, along with other species such as SO₂, NO_x, ammonia, and PM,
68 serve as essential inputs driving air quality model simulations. Uncertainties in VOCs
69 emissions notably impact air quality modelling for O₃, SOA, and total PM_{2.5}. A study
70 conducted in the United States reported substantial underprediction of VOCs emission
71 inventories in urban regions (McDonald et al., 2018), particularly for volatile chemical
72 products (VCPs). A simulation study that developed four cases based on the baseline
73 inventory demonstrated that augmented VOCs emission inventories have notable
74 effects on air pollutants, highlighting the need for more detailed VCPs emissions in the
75 inventory to enhance model performance (Zhu et al., 2019). In China, notable
76 discrepancies in aromatics have been observed between CMAQ predictions and
77 measurements (Wang et al., 2020). Wu et al. (2022) reconciled the bottom-up
78 methodology and measurement constraints to improve the city-scale non-methane
79 VOCs (NMVOCs) emission inventory in Nanjing, resulting in improved O₃ simulation
80 performance with the CMAQ model.

81 Model evaluation serves as the initial step in establishing confidence in air quality
82 model predictions for further analysis. Numerous studies have conducted evaluations
83 of the predicted O₃ and PM_{2.5} concentrations in China (Hu et al., 2016; Li et al., 2021;
84 Li et al., 2020). Overall, the predictions of O₃ and PM_{2.5} concentrations generally align
85 with the observations (Shi et al., 2017; Wang et al., 2021), although substantial biases
86 have been reported in certain circumstances and for specific species, such as O₃ and
87 SOA (Gong et al., 2021; Liu et al., 2020; Hu et al., 2017; Qin et al., 2018). Given that
88 VOCs are key precursors of O₃ and SOA, evaluating VOCs predictions can help
89 elucidate the causes of these substantial biases in predictions. However, VOCs
90 evaluations in regional modelling studies have been infrequent due to limited
91 measurement data. Ambient VOCs have been measured at different locations in China



92 in various studies (Yang et al., 2022; Wang et al., 2022a). Unlike O₃ and PM_{2.5}, which
93 are routinely monitored across major cities and regions in China, VOCs are often
94 measured over short periods at one or specific sites. Different studies may employ
95 different instruments and the study periods may vary, making it challenging to compile
96 VOCs measurement data from multiple studies for a comprehensive model evaluation.
97 In this study, we conducted VOCs evaluations for the first time in China by utilizing
98 summertime observations from 28 sites located in different regions of the country, as
99 part of the "Towards an Air Toxic Management System in China (ATMSYC)" project
100 (Lyu et al., 2020). This study aimed to: (1) assess the disparities in VOC levels between
101 measured ambient concentrations and predicted concentrations in various regions of
102 China using the widely used CMAQ model, (2) quantify the impacts of VOCs species
103 with substantial biases on O₃ predictions through emission adjustments based on
104 observation-prediction differences, and (3) evaluate the sensitivity of O₃ formation to
105 VOCs in key cities, providing recommendations on the necessity of emission
106 inventories and pollution control measures.

107 **2. Materials and Methods**

108 2.1. Observation description

109 The ATMSYC project involved a collaborative sampling campaign at 28 sites in
110 18 cities across China, conducted from 6 June to 24 August, 2018, with speciated VOC
111 measurement as part of the observation task (Lyu et al., 2020). Detailed site information
112 and sampling times can be found in Table S1. Measurements were taken at intervals of
113 two or four hours between 8:00 and 16:00. The collection devices, analytical
114 instruments, quality controls, and other measurement methods have been previously
115 described (Lyu et al., 2019; Lyu et al., 2020; Liu et al., 2021; Zhou et al., 2023). From
116 the ATMSYC dataset, we selected 61 representative VOCs species and classified them



117 into 20 categories, according to the SAPRC07 mechanism (Carter, 2010) to facilitate
118 comparison with model predictions. These species can be categorized into five groups:
119 alkanes, alkenes, aromatics, alkynes, and formaldehydes (HCHO). Further details
120 regarding these specific classifications are mentioned in Table S2.

121 Observations of O₃ and nitrogen dioxide (NO₂) were collected from 28 ground
122 sites, sourced from the Chinese Ministry of Ecology and Environment
123 (<https://www.mee.gov.cn/>, last accessed on 20 April 2022), to assess the simulation
124 performance of the modelled O₃ and NO₂. To evaluate the impact of meteorological
125 conditions, we also collected observation data of meteorological variables (temperature
126 (T2), relative humidity (RH), wind speed (WS) and wind direction (WD)) from the
127 nearest meteorological stations to the 28 sites from the Chinese Meteorological Agency
128 (<http://data.cma.cn/en>, last accessed on 27 April 2022).

129 2.2. Model Configurations

130 The CMAQ version 5.2 model (Appel et al., 2018), coupled with the
131 SAPRC07TIC mechanism and aerosol module AERO6i, was utilized to simulate air
132 quality across China from June to August 2018 (Mao et al., 2022). Meteorological fields
133 were generated using WRF version 4.2.1, employing a 1.0° × 1.0° resolution FNL
134 reanalysis dataset from the National Centre for Atmospheric Research (NCAR). The
135 specific settings of WRF were consistent with those described by Mao et al. (2022), and
136 the simulation performance of the meteorological fields was verified (Mao et al., 2022).
137 The modelling domain with a horizontal resolution of 36 km is shown in Figure 1,
138 which divides China into seven regions: the North China Plain (NCP), Northwest,
139 Northeast, Yangtze River Delta (YRD), Central China, Southwest, and South China
140 (with a higher concentration of sites in the Pearl River Delta (PRD) region).

141 We utilized the Multi-resolution Emission Inventory for China (MEIC) v1.3 with



142 a resolution of $0.25^\circ \times 0.25^\circ$ in 2017 (<http://www.meicmodel.org>, last accessed on 25
143 January 2022) for anthropogenic emissions within China. For anthropogenic emissions
144 outside of China, we employed the Regional Emission Inventory in Asia (REAS) v3.2
145 in 2015 (<https://www.nies.go.jp/REAS/>, last accessed on 25 January 2022). Biogenic
146 emissions were generated using the Model for Emissions of Gases and Aerosols from
147 Nature (MEGAN) v2.1 (Guenther et al., 2012), which were then mapped to 27
148 SAPRC07TIC species, including isoprene (ISOP), α -pinene (APIN), and other BVOCs.
149 Further details on the biogenic emissions can be found in (Li et al., 2022b). Open
150 biomass burning emissions were processed using the Fire Inventory (NCAR FINN,
151 <https://www2.aocom.ucar.edu/modeling/finn-fire-inventory-ncar>, last accessed on 28
152 January 2022).

153 Most emission inventories commonly employ a lumped mechanism to represent
154 VOCs. Li et al. (2014) introduced a method to allocate individual non-methane VOC
155 (NMVOC) emissions in the MEIC inventory to species groups using multiple chemical
156 mechanisms, utilizing mechanism-specific mapping tables from Carter (2013). This
157 method has been widely adopted in CTMs. In this study, we followed this approach and
158 utilized a speciation profile processor called Spec DB, which is available from
159 <https://intra.engr.ucr.edu/~carter/emitdb/>, provided by Carter, to generate the speciation
160 profiles. The mapping scheme for the SAPRC07TIC mechanism in the MEIC and open
161 biomass burning was updated based on the step-by-step assignment framework of the
162 SAPRC07 mechanism provided by the MEIC team.

163 In this study, we examined the performance of CMAQ simulations during the
164 observation period of the ATMSYC project. The days prior to 6 June were considered
165 as a spin-up period. The simulated VOCs values at each site were matched with the
166 observation time to obtain the average concentration during the same period. This



167 duration was defined as the study period.

168 2.3. Adjustment of VOCs emissions

169 Emissions were adjusted for several species that exhibited significant deviations
170 in simulations. The adjustment factors for emissions were determined by calculating
171 the median of the ratio between observed and predicted values at 18 urban sites, which
172 provided an average measure of the deviation for each species. Sensitivity experiments
173 were conducted to examine the impact of the updated VOCs emissions on both
174 predicted VOCs and O₃ levels. To quantify the effect of unit increments in VOCs on O₃
175 concentrations, the Relative Incremental Reactivity (RIR) was calculated. The RIR is a
176 commonly used metric in observation-based model studies (Cardelino and Chameides,
177 1995) to assess the sensitivity of O₃ to individual precursors such as NO_x and various
178 types of VOCs. The calculation of RIR is based on Equation (1):

$$179 \quad RIR(X) = \frac{(N_{O_3}(X) - B_{O_3}(X)) / B_{O_3}(X)}{(N_X(X) - B_X(X)) / B_X(X)} \quad (1)$$

180 In the equation, X represents a specific VOCs species, while B_{O₃} and N_{O₃} represent the
181 O₃ concentrations in the base and adjusted emission case for X, respectively. The
182 denominator on the right-hand side of the equation represents the relative change in
183 emissions after the adjustment for X.

184 3. Results

185 3.1. Model performance evaluation

186 3.1.1. Evaluation of O₃ and NO₂

187 Figure 2 displays the performance of the CMAQ model for the maximum daily 8-
188 hour average (MDA8) O₃ and NO₂ concentrations at 28 sites. Model performance was
189 assessed using statistical parameters, including the normalized mean bias (NMB),
190 normalized mean error (NME), and correlation coefficient (R). The specific values of
191 these statistical metrics can be found in Table S3. The results indicated that the model



192 predictions complied with the observations at most sites in the NCP, Central China, and
193 Southwest, with only slight underpredictions observed at Lanzhou's urban station (LZ-
194 U; NMB = -0.18) and Shanghai's background station (SH-B; NMB = -0.16), and a
195 slight overprediction at Shanghai's urban station (SH-U; NMB = 0.20). However, in the
196 PRD, overpredictions of MDA8 O₃ were observed in locations such as Shenzhen's
197 station (SZ; NMB = 0.39) and Foshan's station (FS; NMB = 0.32), despite the
198 correlation coefficients being higher than the performance criteria at most sites. The
199 CMAQ's NO₂ predictions exhibited underpredictions for most cities in the Northwest,
200 PRD, and some background sites, but substantial overpredictions were evident in
201 certain urban sites, such as Chengdu's urban station (CD-U; NMB = 0.92) and SZ
202 (NMB = 0.52).

203 3.1.2. Evaluation of VOCs

204 Figure 3 presents the observed VOCs concentrations and corresponding CMAQ
205 simulations across all the sites during the observation period. The proportions of the
206 three categorized VOCs groups, namely alkanes, alkenes, and aromatics, are depicted
207 in detail in Figure S1. The results revealed low predicted VOCs concentrations at most
208 sites, with particularly markable underestimation in certain areas. Table S4 displays the
209 mean values of O₃, NO₂, and total VOCs (TVOCs, encompassing the VOCs considered
210 in this study) concentrations at the 28 sites throughout the study period. As indicated in
211 Table 1, the predicted/observed ratio (referred to as ratio hereafter) of TVOCs is $0.74 \pm$
212 0.40 . The underprediction ranged from 2.05 to 50.61 ppbv (5.77% to 85.40%) at 24
213 sites, while overpredictions occurred at four sites, namely SH-U, CU-U, Wuhan's
214 background station (WH-B), and FS, with values ranging from 0.47 to 29.53 ppbv (1.92%
215 to 89.96%). These findings suggested that the CMAQ model, employing the MEIC
216 emission inventory, underpredicted TVOCs concentrations. Notably, the



217 underprediction of TVOCs was more pronounced at sites located in the cities of
218 Lanzhou, Jinan, Shijiazhuang, Guiyang, and Zhengzhou, where TVOCs were
219 underpredicted by factors of two to six.

220 The regional averages of the predicted and observed TVOCs were calculated by
221 averaging the predictions and observations from all the sites in each region (Table S4).
222 The observed ratios of TVOCs predictions varied across regions as follows: YRD
223 (1.04) > Southwest (0.92) > PRD (0.83) > Central China (0.71) > NCP (0.42) >
224 Northwest (0.16). In Figure S2, despite having the highest observed TVOCs value
225 (44.08 ppbv), the model results showed a lower concentration (7.04 ppbv) in the
226 northwest region (specifically in Lanzhou), making it the region with the lowest
227 predicted value. The predicted TVOCs concentration in the YRD region (Shanghai) was
228 the closest to the observed value. However, Figure 3 shows that the VOCs
229 concentrations were notably overpredicted at SH-U and underpredicted at SH-B. The
230 southwest region appeared to have the best performance among all the regions, which
231 could be due to the overpredicted TVOCs at CD-U, which offsets the underprediction
232 at other sites. Overall, the predicted and observed TVOCs concentrations exhibited
233 notable discrepancies in most regions and the performance varied across the regions.

234 Regarding the VOC components shown in Figure S2, alkanes consistently
235 constituted as the most abundant group of VOCs in both observations (38.3% to 50.6%)
236 and predictions (31.6% to 44.9%). This suggested that the predicted proportion of
237 alkanes in TVOCs closely complied with the actual data. Alkenes typically ranked as
238 the second highest VOC component in observations (14.9% to 31.2%), but they were
239 underrepresented in the model (16.5% to 20.0%). In the case of predicted aromatics and
240 HCHO, their proportion in TVOCs often exceeded the observed results, which differed
241 from the alkynes. In terms of absolute concentrations, the underestimation of alkanes



242 and alkenes was relatively pronounced, particularly in the NCP and Northwest regions.
243 The model performed better in predicting the proportions of various VOCs species in
244 the PRD and Southwest regions.

245 Figure 4 illustrates the ratios of O₃, NO₂, and various VOCs species at the 28 sites.
246 The discrepancies in ratios between urban and background sites are presented in Figure
247 S3. The ratio of alkanes is 0.53 ± 0.38 (median \pm standard deviation), indicating an
248 underprediction of 5.65 ± 6.81 ppbv from a concentration standpoint (Table 1). Notably,
249 the alkanes whose reaction rate constant with hydroxyl radical (OH) between 5×10^2
250 and 2.5×10^3 ppm⁻¹ min⁻¹ (ALK2) exhibited the most notable underprediction. The
251 predictions for aromatics showed minor deviations across different sites, but the median
252 ratio was close to one, except for ARO2MN, which was substantially underpredicted
253 with a ratio of 0.31 ± 0.38 (0.32 ± 0.46 at urban sites), and benzene (BENZ), which was
254 2.75 ± 1.97 at urban sites (Table S5). Regarding alkenes, the ratios for the seven alkenes
255 were generally high (0.51 ± 0.48 for alkenes), indicating underprediction in most sites.
256 Particularly, 1,3-butadiene (BDE13) exhibited a notable low ratio, possibly due to its
257 reallocation from the underpredicted alkenes whose reaction rate constant is greater
258 than 7×10^4 ppm⁻¹ min⁻¹ with OH (OLE2) and the allocation factor may not be
259 universally applicable across regions. Furthermore, the predicted content of acetylene
260 (ACYE) was lower at all sites, while the predicted HCHO was slightly overpredicted.
261 Considering that the observed VOCs species primarily originated from anthropogenic
262 emissions and that the majority of emitted VOCs were contributed by the MEIC, the
263 ratios between urban and background sites could verify whether the MEIC emission
264 inventory adequately reflected the differences between urban and background areas.

265 3.2. Adjusting VOCs emissions and their impacts on O₃ predictions

266 These findings indicated a bias between the model-predicted VOCs and observed



267 ambient VOCs concentrations. To evaluate the impact of these biases on O₃ predictions,
268 we modified the VOCs emissions of the MEIC based on the differences between
269 observations and predictions. Previous studies have adjusted emission inventories to
270 match observed constraints for predicting VOCs and O₃ in specific cities (Wu et al.,
271 2022; Wang et al., 2020). Considering the temporal and spatial variability of the 28 sites,
272 we calculated the median ratio of VOCs for the 18 urban sites. We selected coefficients
273 for six representative AVOCs species with deviations exceeding 2.0 times the median,
274 including ALK2, ARO2MN, BENZ, the alkenes (excluding ethene) whose reaction rate
275 constant is less than $7 \times 10^4 \text{ ppm}^{-1} \text{ min}^{-1}$ with OH (OLE1), propene (PRPE), and ACYE,
276 and adjusted their emission rates in the MEIC, resulting in six new cases. Additionally,
277 we conducted a case (case_all) that incorporated the aforementioned adjustments and a
278 case in which NO_x was adjusted by 1.5 based on observational constraints. The
279 adjustment factors for the eight new cases are provided in Table 2.

280 The impact of adjusting VOCs emissions on the concentrations of O₃ and VOCs is
281 presented in Table S6. The underprediction of simulated VOCs and NO₂ values was
282 largely reduced for the new case, as indicated in the six cases with single-species
283 changes and the case_all. In Table S7, the ratio of TVOCs in case_all was modified to
284 0.86 ± 0.47 , demonstrating improved performance in VOCs compared to the base case.
285 However, it was worth noting that even after the emission adjustment, the predicted
286 VOCs concentrations remained lower than the observations (particularly for
287 case_BENZ). This discrepancy resulted from the varying reactivities of different VOC
288 species and NO_x in atmospheric chemical reactions, leading to different levels of
289 depletion. Additionally, both measured and modelled concentrations were subject to
290 photochemical losses (Ma et al., 2022b; Shao et al., 2011). The increased VOCs
291 concentrations resulted in higher O₃ concentrations. Based on the data presented in



292 Tables S6 and S8, the constrained species ALK2, ARO2MN, OLE1, and PRPE, guided
293 by observational data, contributed to an increase in O₃ concentration, especially in
294 case_all, which led to a more pronounced overpredictions ranging from 0.62% to 6.27%
295 across all the sites. In contrast, increasing NO_x had a positive effect and reduced the O₃
296 concentration.

297 To illustrate regional pollution levels on a broader scale, Figure 5 displays the
298 average concentrations of O₃, NO₂, and the six previously mentioned VOCs species
299 studied in China during the specified period.

300 High O₃ levels were particularly prominent in most areas of the NCP, the eastern
301 part of the Northwest, and the Sichuan Basin in the Southwest. NO₂ concentrations
302 were elevated in the NCP, YRD, and PRD regions, as well as in certain megacities. The
303 spatial distribution of various VOCs, derived from TVOCs emissions in the MEIC,
304 exhibited broad consistency, with higher concentrations observed in south-eastern
305 China. Megacities, akin to NO₂, displayed elevated VOCs levels. Different cities
306 exhibited VOCs originating from various sources. ALK2 demonstrated high
307 concentrations in individual cities but less than 1 ppbv in other regions; thus, displaying
308 stronger geographical characteristics compared to the other five VOCs. ARO2MN
309 exhibited the lowest average concentration but exerted a substantial influence on O₃
310 due to its higher reactivity. Figure S4 illustrates the effects of altering the emission rates
311 of NO_x and VOCs in seven scenarios across China. The left panel displays the
312 concentrations in the new cases, while the middle and right panels show the
313 concentration differences for corresponding species and O₃ between the new cases and
314 the base case, respectively. Spatial variations in NO₂ and VOCs exhibited similarities.
315 The increase in NO₂ was more pronounced in the NCP and YRD regions, where NO₂
316 concentrations was consistently high. Previous studies indicate that the NCP and YRD



317 regions are predominantly limited by VOCs during the summer (Li et al., 2017b; Lyu
318 et al., 2019; Liu et al., 2021), resulting in either no change or a reduction in O₃ when
319 NO₂ increases. Conversely, in other areas with low NO₂ concentrations, O₃
320 concentrations increased by 0 to 10 ppbv. BENZ was the only compound whose
321 concentration decreased, and its impact on O₃ in different regions mirrored that of NO₂,
322 albeit at a much lower concentration. The increased emissions of ALK2, ARO2MN,
323 ACYE, OLE1, and PRPE favoured O₃ production, with the most notable effects
324 observed in the NCP, YRD, and other metropolitan areas. Among these compounds,
325 OLE1 exhibited the strongest effect, while ACYE had a minimal influence.

326 The section 2.3 describes the calculation of the RIR values, which were used to
327 demonstrate the sensitivity of the model-simulated O₃ to VOCs constrained by
328 observations in different locations. Figure S5 presents the variations in RIR values for
329 the six VOCs across the 28 sites. OLE1, PRPE, and ARO2MN exhibited a higher RIR
330 values. Urban areas within the same city displayed a higher RIR values compared to
331 the background areas. With the exception of Chengdu, Guiyang, Lanzhou's background
332 station (LZ-B), Guangzhou's background station (GZ-B), and Zhaoqing's station (ZQ),
333 where O₃ generation was more sensitive to PRPE, other areas showed a greater impact
334 of OLE1 concentration on O₃, indicating that adjusting the emission rate of alkenes in
335 the emission inventory was crucial for simulating changes in O₃ concentrations. For
336 instance, improvements could be made in LZ-U, Huizhou's station (HZ), and
337 Jiangmen's station (JM), where O₃ concentrations were underpredicted in the base case.
338 Special attention should be given to the sites with high RIR values such as SH-U, CD-
339 U, SZ, Zhuhai's station (ZH), and others, as O₃ generation in these locations will be
340 highly sensitive to changes in the local VOCs emission inventory. Moreover, ALK2,
341 ACYE, and BENZ had minimal effects on O₃, and BENZ even exhibited a negative



342 RIR values at certain sites.

343 These findings indicated a notable improvement in the underprediction of VOCs
344 when adjustments were made based on VOCs observations. However, the elevated
345 VOCs concentrations in the model could lead to increased O₃ formation, thereby
346 enhancing the model's accuracy in areas where both VOCs and O₃ were underpredicted.
347 Nonetheless, this adjustment will unavoidably worsen any existing overprediction of
348 O₃ in the model.

349 4. **Discussions**

350 4.1. Large bias in TVOCs predictions at specific sites

351 Significant discrepancies between predicted and observed TVOCs were observed
352 in Lanzhou, Jinan, Shijiazhuang, and Zhengzhou. Lanzhou and Shijiazhuang have
353 developed petrochemical industries, where high concentrations of VOCs are frequently
354 detected downwind of industrial areas (Guan et al., 2020; Guo et al., 2022). Figure 3
355 illustrates that alkanes, alkenes, and aromatic were substantially underpredicted due to
356 inadequate prediction of industrial areas with high VOCs emissions in the MEIC. Jinan
357 and Zhengzhou experienced severe air pollution due to heavy industry and traffic
358 (Zhang et al., 2017; Wang et al., 2022c). The simulated levels of TVOCs were
359 substantially lower than the observed levels, with alkenes exhibiting an even greater
360 inaccuracy, being more than 10 times lower in Jinan. At certain sites, the simulated
361 TVOCs exceeded the measurements, including the CD-U, SH-U, WH-B, and FS sites.
362 In CD-U, the predicted TVOCs were almost double the measured values, whereas they
363 were underpredicted in CD-B. In Chengdu, VOCs emissions were dominated by
364 LPG/NG usage and vehicle emissions in summer, with a higher proportion of low-
365 carbon alkanes compared to other cities in China (Xiong et al., 2021). Clearly, the MEIC
366 overpredicted VOCs emissions in CD-U, particularly for HCHO. In SH-U,



367 characterized by a dense population, the simulation of alkenes, aromatics, and HCHO
368 was approximately twice that of the measurements. This aligns with the report
369 by Wang et al. (2020) stating that observation-constrained aromatic emissions were
370 roughly half of the estimates provided by the MEIC in Shanghai, 2015. Peng et al. (2023)
371 also observed inconsistencies between the trend of non-methane hydrocarbon
372 emissions in Shanghai from 2009 to 2015 and the growth trend indicated by the MEIC
373 (Li et al., 2019), suggesting the effectiveness of local pollution control measures.
374 However, SH-B was situated in the easternmost part of Chongming Island, which had
375 the minimal local emissions at the 36 km grid resolution. This likely explains the
376 differences observed between the urban background areas in Shanghai. In the cases of
377 WH-B and FS, which demonstrated excellent model performance for VOCs, only the
378 overprediction of aromatics was more pronounced.

379 Heavy O₃ pollution events, primarily limited by VOCs, have been frequently
380 observed in the PRD region since its rapid development in the last century (Chan et al.,
381 2006; Shao et al., 2009; Li et al., 2014). In the PRD region, slightly lower TVOCs
382 simulations were observed at most sites, primarily due to the underestimation of alkanes
383 and alkenes, while aromatics and HCHO were overestimated. Furthermore, the
384 differences in VOCs components among the cities in the PRD region could be attributed
385 to local industry characteristics, and variations in prevention and control policies. For
386 instance, observed ethene (ETHE) in FS accounted for over 50% of the alkenes,
387 whereas simulations accounted for only 35%. The predicted ETHE ratio in ZH was
388 higher (50%) than the observed ratio (20%), while other cities exhibited similar ETHE
389 percentages. Moreover, the proportion of ISOP in Guangzhou's alkenes was higher than
390 that in other PRD cities, suggesting effective control of local anthropogenic alkene
391 emissions, consistent with the findings of Zhao et al. (2022).



392 4.2. Urban-background evaluation

393 Differences in atmospheric VOCs among urban background areas have been
394 extensively demonstrated (Sillman, 1999; Shao et al., 2020). As depicted in Figure 6,
395 we compared the average performance of the model for 18 urban sites and 10
396 background sites. In urban areas, the predicted TVOCs concentration (23.76 ppbv) was
397 lower than the observed concentration (32.46 ppbv), primarily due to the
398 underprediction of alkanes, alkenes, and alkynes. Predicted aromatics and HCHO
399 exhibited higher proportions and concentrations compared to the observations. In the
400 background areas, TVOCs were also underpredicted, with concentrations lower than
401 those in urban areas, as indicated by both the observed and predicted values. Each of
402 the five VOCs showed lower predictions, with alkanes exhibiting the most notable
403 disparity, with a decrease of 6.91 ppbv compared to the observed values. This suggested
404 that the model underpredicted alkanes in urban areas, which were predominantly
405 derived from the petrochemical industry or fuel evaporation (Wang et al., 2022a). The
406 predicted proportions of alkanes, aromatics, and HCHO exhibited urban-background
407 differences consistent with the observations, reflecting the characteristics of urban and
408 background areas in the model. These differences were well represented in our
409 horizontal grid resolution of only 36 km. Overall, the CMAQ model captured the
410 characteristics of different regions and urban background areas but underestimated the
411 concentrations of certain individual VOC species.

412 The ratios distinguished between urban and background areas are presented in
413 Figure S3. The comparison revealed that the alkanes were more prominently
414 underpredicted in the background area than in the urban area. Xylene (XYL), 1,2,4-
415 trimethylbenzene (B124), OLE1, OLE2, and PRPE were also underpredicted to a
416 greater extent in the background area. This could be attributed to the scarcity of



417 background sites or the model's underprediction of VOCs emissions in the background
418 area. The model's performance in simulating ISOP, a BVOC, in urban areas was not as
419 satisfactory as in the background areas, which was consistent with the findings of Ma
420 et al. (2021) suggesting that MEGAN could underestimate the emissions from urban
421 green spaces. APIN, a notable monoterpene, including anthropogenic emissions from
422 biomass burning and VCPs, could be either underpredicted or disregarded (Wang et al.,
423 2022b; McDonald et al., 2018), resulting in common underprediction with a median
424 ratio of five in urban-background areas. Additionally, the simulated HCHO
425 concentrations were higher in the urban areas. Overall, these results indicated that the
426 model generally performed better for anthropogenic VOCs in the urban areas. However,
427 there were still a few notable outliers and significant deviations for a majority of VOCs,
428 particularly those with high chemical reactivity. These deviations will inevitably impact
429 the model's calculation of photochemical reactions involved in O₃ generation.

430 4.3. Implications and suggestions

431 Accurately predicting VOCs is crucial for O₃ modelling. However, due to limited
432 measurement data and uncertainties in emission inventories, accurately simulating the
433 VOCs across China using CTMs remains challenging.

434 Considerable efforts have been dedicated to the development of VOCs emission
435 inventories in recent years (Li et al., 2019; An et al., 2021; Chang et al., 2022). However,
436 our findings indicate substantial variation in the model performance of VOCs across
437 different regions and species. Therefore, the inclusion of accurate local emission factors,
438 activity data, and source profiles is essential. Sha et al. (2021) compiled an integrated
439 dataset of AVOCs source profiles in China, emphasizing the need for supplementary
440 and timely updates to these profiles in the future. Apart from anthropogenic emissions,
441 model resolution, and chemical mechanisms meteorological conditions, and BVOCs



442 emissions also contribute to the uncertainty of VOCs modelling, thereby affecting the
443 performance of O₃ modelling (Zhang et al., 2021; Wang et al., 2021; Liu et al., 2022).

444 High-resolution models require higher emission inventory resolution (Li et al.,
445 2022; An et al., 2021), which can improve simulation performance to a certain extent.

446 Given the large scope of the model used in this study and the 0.25° × 0.25° horizontal
447 resolution of the MEIC inventory, a resolution of 36 km was chosen to balance
448 computational efficiency and the preservation of information from the emission
449 inventory, but inevitably results in deviation of the modelled VOCs and other elements.

450 On the one hand, urban and background sites in close proximity may be assigned to the
451 same grid in the model, as shown in Table S3, making it difficult to distinguish the
452 differences in modelled VOCs between urban and background sites in cities such as
453 Shijiazhuang, Jinan, Wuhan, and Guiyang; on the other hand, in real atmospheres, even
454 with close proximity, the observed VOCs may differ greatly in concentration, which is
455 challenging to capture in a coarse-resolution model. When applying coarse-resolution
456 emission inventories, increasing the model resolution can enhance the spatial
457 correlation between observed and predicted concentrations, but does not always
458 improve simulation performance (Zheng et al., 2021). High-resolution models may
459 introduce more emission mapping errors, which can be reduced by using coarse-
460 resolution model grids (Zheng et al., 2021). Therefore, addressing this issue requires
461 not only finer model resolution but also improved emission inventories.

462 The SAPRC07tic chemical mechanism used in this study has been proven reliable
463 in previous model applications (Qin et al., 2022), reducing the computational effort
464 compared to the explicit MCM mechanism (Li et al., 2015) while retaining the chemical
465 reactivity of various VOCs. However, the lumped VOCs species contain more VOCs
466 species than those in corresponding observations. Therefore, if both the emission



467 inventory and model are sufficiently accurate, the predicted values should theoretically
468 be higher.

469 Meteorology bias also contributed to some bias of the VOCs predictions. We added
470 evaluation of the meteorology predictions in this study, and the results are shown in
471 Table S9 and S10. The results are consistent with other studies in China (Mao et al.,
472 2022; Wang et al., 2021). It is observed that temperature is overpredicted at most sites,
473 while RH is mostly underpredicted. The combination of high temperature and low RH
474 facilitates the consumption of VOCs through photochemical reactions, which may
475 explain the tendency of our modelled VOCs to be underestimated. But we believe it is
476 insufficient to account for the underestimation of low-reactivity VOC species (mainly
477 alkanes). Furthermore, the modelled wind speeds slightly exceed the observations,
478 which may also contribute to VOCs underprediction (Table S10). While the bias in
479 meteorological conditions contributes to the underestimation of modelled VOCs, the
480 underestimated VOCs emissions is the key factor for the VOCs underprediction across
481 most of the cities.

482 In this study, the adjustment of VOCs emissions resulted in increased predicted
483 emission levels, subsequently leading to higher O₃ predictions. However, these
484 adjustments are simplistic and fail to account for regional variations in VOCs biases.
485 The accuracy of VOCs measurement data is also crucial. Therefore, there is a need to
486 promote the establishment of a national O₃ precursor monitoring network and develop
487 a standardized framework with quality control systems. This would facilitate the
488 comparability of VOCs measurements between regions, thereby supporting related
489 research and the implementation of collaborative regional prevention and control
490 measures.

491 **5. Conclusion**



492 In this study, we conducted a comprehensive evaluation of the simulation
493 performance of VOCs using the CMAQ model and investigated the influence of
494 predicted VOCs on O₃ formation. The inclusion of summertime-observed VOCs data
495 from the ATMSYC project for 28 sites in China enhanced the spatiotemporal
496 comparability of our model evaluation.

497 During the study period, TVOCs were found to be underpredicted by 14.1 ± 13.2
498 ppbv at 24 sites, except for SH-U, CD-U, WH-B, and FS. Despite some sites exhibiting
499 similar TVOCs concentrations, differences still persisted in their specific components.
500 Through considering the uncertainties of the MEIC model and relevant factors, we
501 found several sites with substantial inaccuracies, such as Jinan, Shijiazhuang, Lanzhou,
502 Chengdu, and Guiyang. The model's performance in predicting TVOCs and their
503 components varied across regions, with better predictions observed in urban areas
504 compared to background areas.

505 Alkanes, alkenes, ARO2MN, and alkynes are generally underpredicted, with ratios
506 of 0.53 ± 0.38 , 0.51 ± 0.48 , 0.31 ± 0.38 , and 0.41 ± 0.47 , respectively. In urban areas,
507 the CMAQ model exhibited underpredictions for OLE1, ALK2, ARO2MN, PRPE,
508 ACYE, and NO_x, ranging from 2.0 to 4.6 times, while overpredicting BENZ by 2.75
509 times. For sensitivity experiments, their emissions were adjusted and their impact on
510 O₃ and VOCs was evaluated. These adjustments improved the model's VOCs
511 performance, resulting in a change in the ratio of total VOCs to 0.86 ± 0.47 . However,
512 the increased VOCs contributed to higher reactivity, exacerbating O₃ overpredictions
513 by 0.62% to 6.27% across the sites. Consequently, RIR values were calculated to depict
514 the varying reactivities of VOCs in different regions, with OLE1, PRPE, and ARO2MN
515 contributing the highest RIR values during the study period.

516 Due to the inaccuracies present in current VOCs emission inventories, notable



517 efforts are needed to enhance the development and updating of emission inventories,
518 particularly in regions characterized by developed industries, evolving energy
519 structures, and relatively underdeveloped conditions. It is only through improving the
520 accuracy of VOCs emission inventories that we can ensure reliable model performance
521 in predicting O₃ levels, thereby establishing a solid foundation for addressing the
522 escalating issue of O₃ pollution.

523

524 **Code and data availability**

525 The model outputs and observation data are currently available upon request.

526 **Author contributions**

527 YS and JH designed research. YS, JH, JL, MQ, XX, KG, FY, and JM contributed to
528 model development, simulations, and data processing. XL and HG provided the
529 observation data. XL and LH contributed to result discussion. YS prepared the
530 manuscript and all coauthors helped improve the manuscript.

531 **Competing interests**

532 The authors declare that they have no conflict of interest.

533 **Acknowledgements**

534 This work was supported by the National Natural Science Foundation of China
535 (42007187, 42021004, 42277095).

536



537 References

- 538 An, J., Huang, Y., Huang, C., Wang, X., Yan, R., Wang, Q., Wang, H., Jing, S., Zhang, Y., Liu, Y., Chen,
539 Y., Xu, C., Qiao, L., Zhou, M., Zhu, S., Hu, Q., Lu, J., and Chen, C.: Emission inventory of air pollutants
540 and chemical speciation for specific anthropogenic sources based on local measurements in the
541 Yangtze River Delta region, China, *Atmos. Chem. Phys.*, 21, 2003-2025, 10.5194/acp-21-2003-
542 2021, 2021.
- 543 Appel, W., Napelenok, S., Hogrefe, C., Pouliot, G., Foley, K. M., Roselle, S. J., Pleim, J. E., Bash, J.,
544 Pye, H. O. T., Heath, N., Murphy, B., and Mathur, R.: Overview and Evaluation of the Community
545 Multiscale Air Quality (CMAQ) Modeling System Version 5.2, *Air Pollution Modeling and its
546 Application XXV*, Cham, 69-73,
- 547 Cardelino, C. A. and Chameides, W. L.: An observation-based model for analyzing ozone precursor
548 relationships in the urban atmosphere, *J Air Waste Manag Assoc*, 45, 161-180,
549 10.1080/10473289.1995.10467356, 1995.
- 550 Carter, W. P. L.: Development of the SAPRC-07 chemical mechanism, *Atmospheric Environment*,
551 44, 5324-5335, 10.1016/j.atmosenv.2010.01.026, 2010.
- 552 Carter, W. P. L.: Development of an improved chemical speciation database for processing
553 emissions of volatile organic compounds for air quality models, report available at:
554 <https://intra.engr.ucr.edu/~carter/emitdb/>, 2013.
- 555 Chan, L., Chu, K., Zou, S., Chan, C., Wang, X., Barletta, B., Blake, D., Guo, H., and Tsai, W.:
556 Characteristics of nonmethane hydrocarbons (NMHCs) in industrial, industrial-urban, and
557 industrial-suburban atmospheres of the Pearl River Delta (PRD) region of south China, *Journal of
558 Geophysical Research*, 111, 10.1029/2005jd006481, 2006.
- 559 Chang, X., Zhao, B., Zheng, H., Wang, S., Cai, S., Guo, F., Gui, P., Huang, G., Wu, D., Han, L., Xing,
560 J., Man, H., Hu, R., Liang, C., Xu, Q., Qiu, X., Ding, D., Liu, K., Han, R., Robinson, A. L., and Donahue,
561 N. M.: Full-volatility emission framework corrects missing and underestimated secondary organic
562 aerosol sources, *One Earth*, 5, 403-412, 10.1016/j.oneear.2022.03.015, 2022.
- 563 Dang, R., Liao, H., and Fu, Y.: Quantifying the anthropogenic and meteorological influences on
564 summertime surface ozone in China over 2012-2017, *Sci Total Environ*, 754, 142394,
565 10.1016/j.scitotenv.2020.142394, 2021.
- 566 Emery, C., Liu, Z., Russell, A. G., Odman, M. T., Yarwood, G., and Kumar, N.: Recommendations on
567 statistics and benchmarks to assess photochemical model performance, *J Air Waste Manag Assoc*,
568 67, 582-598, 10.1080/10962247.2016.1265027, 2017.
- 569 Gong, K., Li, L., Li, J., Qin, M., Wang, X., Ying, Q., Liao, H., Guo, S., Hu, M., Zhang, Y., and Hu, J.:
570 Quantifying the impacts of inter-city transport on air quality in the Yangtze River Delta urban
571 agglomeration, China: Implications for regional cooperative controls of PM_{2.5} and O₃, *Sci Total
572 Environ*, 779, 146619, 10.1016/j.scitotenv.2021.146619, 2021.
- 573 Guan, Y., Wang, L., Wang, S., Zhang, Y., Xiao, J., Wang, X., Duan, E., and Hou, L.: Temporal variations
574 and source apportionment of volatile organic compounds at an urban site in Shijiazhuang, China,
575 *J Environ Sci (China)*, 97, 25-34, 10.1016/j.jes.2020.04.022, 2020.
- 576 Guenther, A., Karl, T., Harley, P., Wiedinmyer, C., Palmer, P. I., and Geron, C.: Estimates of global
577 terrestrial isoprene emissions using MEGAN (Model of Emissions of Gases and Aerosols from
578 Nature), *Atmos. Chem. Phys.*, 6, 3181-3210, 10.5194/acp-6-3181-2006, 2006.
- 579 Guenther, A., Jiang, X., Heald, C., Sakulyanontvittaya, T., Duhl, T., Emmons, L., and Wang, X.: The
580 Model of Emissions of Gases and Aerosols from Nature version 2.1 (MEGAN2.1): an extended and
581 updated framework for modeling biogenic emissions, *Geoscientific Model Development*, 5, 1471-
582 1492, 10.5194/gmd-5-1471-2012, 2012.
- 583 Guo, W., Yang, Y., Chen, Q., Zhu, Y., Zhang, Y., Zhang, Y., Liu, Y., Li, G., Sun, W., and She, J.: Chemical
584 reactivity of volatile organic compounds and their effects on ozone formation in a petrochemical
585 industrial area of Lanzhou, Western China, *Sci Total Environ*, 839, 155901,
586 10.1016/j.scitotenv.2022.155901, 2022.



- 587 Hu, J., Chen, J., Ying, Q., and Zhang, H.: One-year simulation of ozone and particulate matter in
588 China using WRF/CMAQ modeling system, *Atmospheric Chemistry and Physics*, 16, 10333-10350,
589 10.5194/acp-16-10333-2016, 2016.
- 590 Hu, J., Wang, P., Ying, Q., Zhang, H., Chen, J., Ge, X., Li, X., Jiang, J., Wang, S., Zhang, J., Zhao, Y.,
591 and Zhang, Y.: Modeling biogenic and anthropogenic secondary organic aerosol in China,
592 *Atmospheric Chemistry and Physics*, 17, 77-92, 10.5194/acp-17-77-2017, 2017.
- 593 Kelly, J. M., Doherty, R. M., O'Connor, F. M., and Mann, G. W.: The impact of biogenic,
594 anthropogenic, and biomass burning volatile organic compound emissions on regional and
595 seasonal variations in secondary organic aerosol, *Atmospheric Chemistry and Physics*, 18, 7393-
596 7422, 10.5194/acp-18-7393-2018, 2018.
- 597 Kroll, J. H. and Seinfeld, J. H.: Chemistry of secondary organic aerosol: Formation and evolution of
598 low-volatility organics in the atmosphere, *Atmospheric Environment*, 42, 3593-3624,
599 10.1016/j.atmosenv.2008.01.003, 2008.
- 600 Kurokawa, J. and Ohara, T.: Long-term historical trends in air pollutant emissions in Asia: Regional
601 Emission inventory in ASia (REAS) version 3, *Atmos. Chem. Phys.*, 20, 12761-12793, 10.5194/acp-
602 20-12761-2020, 2020.
- 603 Li, C., Liu, Y., Cheng, B., Zhang, Y., Liu, X., Qu, Y., An, J., Kong, L., Zhang, Y., Zhang, C., Tan, Q., and
604 Feng, M.: A comprehensive investigation on volatile organic compounds (VOCs) in 2018 in Beijing,
605 China: Characteristics, sources and behaviours in response to O₃ formation, *Sci Total Environ*, 806,
606 150247, 10.1016/j.scitotenv.2021.150247, 2022a.
- 607 Li, J., Cleveland, M., Ziemba, L. D., Griffin, R. J., Barsanti, K. C., Pankow, J. F., and Ying, Q.: Modeling
608 regional secondary organic aerosol using the Master Chemical Mechanism, *Atmospheric
609 Environment*, 102, 52-61, 10.1016/j.atmosenv.2014.11.054, 2015.
- 610 Li, J., Lu, K., Lv, W., Li, J., Zhong, L., Ou, Y., Chen, D., Huang, X., and Zhang, Y.: Fast increasing of
611 surface ozone concentrations in Pearl River Delta characterized by a regional air quality monitoring
612 network during 2006–2011, *Journal of Environmental Sciences*, 26, 23-36, 10.1016/s1001-
613 0742(13)60377-0, 2014.
- 614 Li, J., Xie, X., Li, L., Wang, X., Wang, H., Jing, S., Ying, Q., Qin, M., and Hu, J.: Fate of Oxygenated
615 Volatile Organic Compounds in the Yangtze River Delta Region: Source Contributions and Impacts
616 on the Atmospheric Oxidation Capacity, *Environ Sci Technol*, 56, 11212-11224,
617 10.1021/acs.est.2c00038, 2022b.
- 618 Li, K., Jacob, D. J., Shen, L., Lu, X., De Smedt, I., and Liao, H.: Increases in surface ozone pollution in
619 China from 2013 to 2019: anthropogenic and meteorological influences, *Atmospheric Chemistry
620 and Physics*, 20, 11423-11433, 10.5194/acp-20-11423-2020, 2020.
- 621 Li, K., Chen, L., Ying, F., White, S. J., Jang, C., Wu, X., Gao, X., Hong, S., Shen, J., Azzi, M., and Cen,
622 K.: Meteorological and chemical impacts on ozone formation: A case study in Hangzhou, China,
623 *Atmospheric Research*, 196, 40-52, 10.1016/j.atmosres.2017.06.003, 2017b.
- 624 Li, L., Xie, F., Li, J., Gong, K., Xie, X., Qin, Y., Qin, M., and Hu, J.: Diagnostic analysis of regional ozone
625 pollution in Yangtze River Delta, China: A case study in summer 2020, *Sci Total Environ*, 812,
626 151511, 10.1016/j.scitotenv.2021.151511, 2022.
- 627 Li, L., Hu, J., Li, J., Gong, K., Wang, X., Ying, Q., Qin, M., Liao, H., Guo, S., Hu, M., and Zhang, Y.:
628 Modelling air quality during the EXPLORE-YRD campaign – Part II. Regional source apportionment
629 of ozone and PM_{2.5}, *Atmospheric Environment*, 247, 10.1016/j.atmosenv.2020.118063, 2021.
- 630 Li, M., Liu, H., Geng, G., Hong, C., Liu, F., Song, Y., Tong, D., Zheng, B., Cui, H., Man, H., Zhang, Q.,
631 and He, K.: Anthropogenic emission inventories in China: a review, *National Science Review*, 4,
632 834-866, 10.1093/nsr/nwx150, 2017a.
- 633 Li, M., Zhang, Q., Zheng, B., Tong, D., Lei, Y., Liu, F., Hong, C., Kang, S., Yan, L., Zhang, Y., Bo, Y., Su,
634 H., Cheng, Y., and He, K.: Persistent growth of anthropogenic non-methane volatile organic
635 compound (NMVOC) emissions in China during 1990–2017: drivers, speciation and ozone
636 formation potential, *Atmospheric Chemistry and Physics*, 19, 8897-8913, 10.5194/acp-19-8897-
637 2019, 2019.



- 638 Liu, T., Wang, C., Wang, Y., Huang, L., Li, J., Xie, F., Zhang, J., and Hu, J.: Impacts of model resolution
639 on predictions of air quality and associated health exposure in Nanjing, China, *Chemosphere*, 249,
640 126515, 10.1016/j.chemosphere.2020.126515, 2020.
- 641 Liu, X., Guo, H., Zeng, L., Lyu, X., Wang, Y., Zeren, Y., Yang, J., Zhang, L., Zhao, S., Li, J., and Zhang,
642 G.: Photochemical ozone pollution in five Chinese megacities in summer 2018, *Sci Total Environ*,
643 801, 149603, 10.1016/j.scitotenv.2021.149603, 2021.
- 644 Liu, Y., Li, J., Ma, Y., Zhou, M., Tan, Z., Zeng, L., Lu, K., and Zhang, Y.: A review of gas-phase chemical
645 mechanisms commonly used in atmospheric chemistry modelling, *Journal of Environmental*
646 *Sciences*, <https://doi.org/10.1016/j.jes.2022.10.031>, 2022.
- 647 Lyu, X., Wang, N., Guo, H., Xue, L., Jiang, F., Zeren, Y., Cheng, H., Cai, Z., Han, L., and Zhou, Y.:
648 Causes of a continuous summertime O₃ pollution event in Jinan, a central
649 city in the North China Plain, *Atmospheric Chemistry and Physics*, 19, 3025–3042, 10.5194/acp-
650 19-3025-2019, 2019.
- 651 Lyu, X., Guo, H., Wang, Y., Zhang, F., Nie, K., Dang, J., Liang, Z., Dong, S., Zeren, Y., Zhou, B., Gao,
652 W., Zhao, S., and Zhang, G.: Hazardous volatile organic compounds in ambient air of China,
653 *Chemosphere*, 246, 125731, 10.1016/j.chemosphere.2019.125731, 2020.
- 654 Ma, M., Gao, Y., Ding, A., Su, H., Liao, H., Wang, S., Wang, X., Zhao, B., Zhang, S., Fu, P., Guenther,
655 A. B., Wang, M., Li, S., Chu, B., Yao, X., and Gao, H.: Development and Assessment of a High-
656 Resolution Biogenic Emission Inventory from Urban Green Spaces in China, *Environ Sci Technol*,
657 56, 175–184, 10.1021/acs.est.1c06170, 2021.
- 658 Ma, W., Feng, Z., Zhan, J., Liu, Y., Liu, P., Liu, C., Ma, Q., Yang, K., Wang, Y., He, H., Kulmala, M., Mu,
659 Y., and Liu, J.: Influence of photochemical loss of volatile organic compounds on understanding
660 ozone formation mechanism, *Atmospheric Chemistry and Physics*, 22, 4841–4851, 10.5194/acp-
661 22-4841-2022, 2022b.
- 662 Mao, J., Li, L., Li, J., Sulaymon, I. D., Xiong, K., Wang, K., Zhu, J., Chen, G., Ye, F., Zhang, N., Qin, Y.,
663 Qin, M., and Hu, J.: Evaluation of Long-Term Modeling Fine Particulate Matter and Ozone in China
664 During 2013–2019, *Frontiers in Environmental Science*, 10, 10.3389/fenvs.2022.872249, 2022.
- 665 McDonald, B. C., de Gouw, J. A., Gilman, J. B., Jathar, S. H., Akherati, A., Cappa, C. D., Jimenez, J. L.,
666 Lee-Taylor, J., Hayes, P. L., McKeen, S. A., Cui, Y. Y., Kim, S.-W., Gentner, D. R., Isaacman-VanWertz,
667 G., Goldstein, A. H., Harley, R. A., Frost, G. J., Roberts, J. M., Ryerson, T. B., and Trainer, M.: Volatile
668 chemical products emerging as largest petrochemical source of urban organic emissions, *Science*,
669 359, 760–764, 10.1126/science.aaq0524, 2018.
- 670 Peng, Y., Wang, H., Wang, Q., Jing, S., An, J., Gao, Y., Huang, C., Yan, R., Dai, H., Cheng, T., Zhang,
671 Q., Li, M., Hu, J., Shi, Z., Li, L., Lou, S., Tao, S., Hu, Q., Lu, J., and Chen, C.: Observation-based sources
672 evolution of non-methane hydrocarbons (NMHCs) in a megacity of China, *J Environ Sci (China)*,
673 124, 794–805, 10.1016/j.jes.2022.01.040, 2023.
- 674 Qin, M., Hu, A., Mao, J., Li, X., Sheng, L., Sun, J., Li, J., Wang, X., Zhang, Y., and Hu, J.: PM_{2.5} and
675 O₃ relationships affected by the atmospheric oxidizing capacity in the Yangtze River Delta, China,
676 *Sci Total Environ*, 810, 152268, 10.1016/j.scitotenv.2021.152268, 2022.
- 677 Qin, M., Hu, Y., Wang, X., Vasilakos, P., Boyd, C. M., Xu, L., Song, Y., Ng, N. L., Nenes, A., and Russell,
678 A. G.: Modeling biogenic secondary organic aerosol (BSOA) formation from monoterpene
679 reactions with NO₃: A case study of the SOAS campaign using CMAQ, *Atmospheric Environment*,
680 184, 146–155, 10.1016/j.atmosenv.2018.03.042, 2018.
- 681 Sha, Q., Zhu, M., Huang, H., Wang, Y., Huang, Z., Zhang, X., Tang, M., Lu, M., Chen, C., Shi, B., Chen,
682 Z., Wu, L., Zhong, Z., Li, C., Xu, Y., Yu, F., Jia, G., Liao, S., Cui, X., Liu, J., and Zheng, J.: A newly
683 integrated dataset of volatile organic compounds (VOCs) source profiles and implications for the
684 future development of VOCs profiles in China, *Sci Total Environ*, 793, 148348,
685 10.1016/j.scitotenv.2021.148348, 2021.
- 686 Shao, M., Wang, B., Lu, S., Yuan, B., and Wang, M.: Effects of Beijing Olympics Control Measures
687 on Reducing Reactive Hydrocarbon Species, *Environ. Sci. Technol.*, 45, 514–519, 2011.
- 688 Shao, M., Zhang, Y., Zeng, L., Tang, X., Zhang, J., Zhong, L., and Wang, B.: Ground-level ozone in



- 689 the Pearl River Delta and the roles of VOC and NO_x in its production, *Journal of Environmental*
690 *Management*, 90, 512-518, 10.1016/j.jenvman.2007.12.008, 2009.
- 691 Shao, P., Xu, X., Zhang, X., Xu, J., Wang, Y., and Ma, Z.: Impact of volatile organic compounds and
692 photochemical activities on particulate matters during a high ozone episode at urban, suburb and
693 regional background stations in Beijing, *Atmospheric Environment*, 236,
694 10.1016/j.atmosenv.2020.117629, 2020.
- 695 Shi, Z., Li, J., Huang, L., Wang, P., Wu, L., Ying, Q., Zhang, H., Lu, L., Liu, X., Liao, H., and Hu, J.:
696 Source apportionment of fine particulate matter in China in 2013 using a source-oriented chemical
697 transport model, *Sci Total Environ*, 601-602, 1476-1487, 10.1016/j.scitotenv.2017.06.019, 2017.
- 698 Sillman, S.: The relation between ozone, NO_x and hydrocarbons in urban and polluted rural
699 environments, *Atmos. Environ.*, 33 1821–1845, 10.1016/S1352-2310(98)00345-8, 1999.
- 700 Wang, G., Zhao, N., Zhang, H., Li, G., and Xin, G.: Spatiotemporal Distributions of Ambient Volatile
701 Organic Compounds in China: Characteristics and Sources, *Aerosol and Air Quality Research*, 22,
702 10.4209/aaqr.210379, 2022a.
- 703 Wang, H., Ma, X., Tan, Z., Wang, H., Chen, X., Chen, S., Gao, Y., Liu, Y., Liu, Y., Yang, X., Yuan, B.,
704 Zeng, L., Huang, C., Lu, K., and Zhang, Y.: Anthropogenic monoterpenes aggravating ozone
705 pollution, *National Science Review*, 9, 10.1093/nsr/nwac103, 2022b.
- 706 Wang, H., Yan, R., Xu, T., Wang, Y., Wang, Q., Zhang, T., An, J., Huang, C., Gao, Y., Gao, Y., Li, X.,
707 Yu, C., Jing, S., Qiao, L., Lou, S., Tao, S., and Li, Y.: Observation Constrained Aromatic Emissions in
708 Shanghai, China, *Journal of Geophysical Research: Atmospheres*, 125, 10.1029/2019jd031815,
709 2020.
- 710 Wang, X., Yin, S., Zhang, R., Yuan, M., and Ying, Q.: Assessment of summertime O₃ formation and
711 the O₃-NO_x-VOC sensitivity in Zhengzhou, China using an observation-based model, *Sci Total*
712 *Environ*, 813, 152449, 10.1016/j.scitotenv.2021.152449, 2022c.
- 713 Wang, X., Li, L., Gong, K., Mao, J., Hu, J., Li, J., Liu, Z., Liao, H., Qiu, W., Yu, Y., Dong, H., Guo, S., Hu,
714 M., Zeng, L., and Zhang, Y.: Modelling air quality during the EXPLORE-YRD campaign – Part I.
715 Model performance evaluation and impacts of meteorological inputs and grid resolutions,
716 *Atmospheric Environment*, 246, 10.1016/j.atmosenv.2020.118131, 2021.
- 717 Wu, R., Zhao, Y., Xia, S., Hu, W., Xie, F., Zhang, Y., Sun, J., Yu, H., An, J., and Wang, Y.: Reconciling
718 the bottom-up methodology and ground measurement constraints to improve the city-scale
719 NMVOCs emission inventory: A case study of Nanjing, China, *Science of The Total Environment*,
720 812, 10.1016/j.scitotenv.2021.152447, 2022.
- 721 Xiong, C., Wang, N., Zhou, L., Yang, F., Qiu, Y., Chen, J., Han, L., and Li, J.: Component characteristics
722 and source apportionment of volatile organic compounds during summer and winter in downtown
723 Chengdu, southwest China, *Atmospheric Environment*, 258, 10.1016/j.atmosenv.2021.118485,
724 2021.
- 725 Yang, Y., Liu, B., Hua, J., Yang, T., Dai, Q., Wu, J., Feng, Y., and Hopke, P. K.: Global review of source
726 apportionment of volatile organic compounds based on highly time-resolved data from 2015 to
727 2021, *Environ Int*, 165, 107330, 10.1016/j.envint.2022.107330, 2022.
- 728 Zhang, G., Wang, N., Jiang, X., and Zhao, Y.: Characterization of Ambient Volatile Organic
729 Compounds (VOCs) in the Area Adjacent to a Petroleum Refinery in Jinan, China, *Aerosol and Air*
730 *Quality Research*, 17, 944-950, 10.4209/aaqr.2016.07.0303, 2017.
- 731 Zhang, M., Zhao, C., Yang, Y., Du, Q., Shen, Y., Lin, S., Gu, D., Su, W., and Liu, C.: Modeling
732 sensitivities of BVOCs to different versions of MEGAN emission schemes in WRF-Chem (v3.6) and
733 its impacts over eastern China, *Geoscientific Model Development*, 14, 6155-6175, 10.5194/gmd-
734 14-6155-2021, 2021.
- 735 Zhang, Q., Streets, D. G., Carmichael, G. R., He, K. B., Huo, H., Kannari, A., Klimont, Z., Park, I. S.,
736 Reddy, S., Fu, J. S. J. A. c., and physics: Asian emissions in 2006 for the NASA INTEX-B mission,
737 *Atmos. Chem. Phys.*, 9, 5131–5153, 10.5194/acp-9-5131-2009, 2009.
- 738 Zhao, M., Zhang, Y., Pei, C., Chen, T., Mu, J., Liu, Y., Wang, Y., Wang, W., and Xue, L.: Worsening
739 ozone air pollution with reduced NO_x and VOCs in the Pearl River Delta region in autumn 2019:



740 Implications for national control policy in China, *J Environ Manage*, 324, 116327,
741 10.1016/j.jenvman.2022.116327, 2022.
742 Zheng, B., Cheng, J., Geng, G., Wang, X., Li, M., Shi, Q., Qi, J., Lei, Y., Zhang, Q., and He, K.: Mapping
743 anthropogenic emissions in China at 1 km spatial resolution and its application in air quality
744 modeling, *Sci Bull (Beijing)*, 66, 612–620, 10.1016/j.scib.2020.12.008, 2021.
745 Zhou, B., Guo, H., Zeren, Y., Wang, Y., Lyu, X., Wang, B., and Wang, H.: An Observational Constraint
746 of VOC Emissions for Air Quality Modeling Study in the Pearl River Delta Region, *Journal of*
747 *Geophysical Research: Atmospheres*, 128, 10.1029/2022jd038122, 2023.
748 Zhu, S., Kinnon, M. M., Shaffer, B. P., Samuelsen, G. S., Brouwer, J., and Dabdub, D.: An uncertainty
749 for clean air: Air quality modeling implications of underestimating VOC emissions in urban
750 inventories, *Atmospheric Environment*, 211, 256–267, 10.1016/j.atmosenv.2019.05.019, 2019.
751



752 Table 1. Mean, median, maximum (max), minimum (min), and standard deviation (std)

753 of the Ratios and differences (Diff) for five VOCs groups and TVOCs at 28 sites

		Alkanes	Alkenes	Aromatics	ARO2MN (Aromatics)	Alkyne	HCHO	TVOCs
Ratio(pre/obs)	mean	0.59	0.60	1.33	0.40	0.55	1.66	0.70
	median	0.53	0.51	1.30	0.31	0.41	1.21	0.74
	max	1.87	2.46	3.29	1.96	2.36	8.70	1.90
	min	0.13	0.09	0.10	0.05	0.09	0.25	0.15
	std	0.38	0.48	0.89	0.38	0.47	1.61	0.40
Diff(pre-obs)	mean	-6.18	-4.02	0.42	-0.28	-1.16	0.16	-10.78
	median	-5.65	-2.56	0.83	-0.25	-1.04	0.49	-7.57
	max	14.12	3.50	6.09	0.24	0.87	5.57	29.53
	min	-19.40	-15.50	-8.18	-0.74	-2.64	-8.90	-50.61
	std	6.81	4.69	3.47	0.20	0.97	2.99	16.11

754

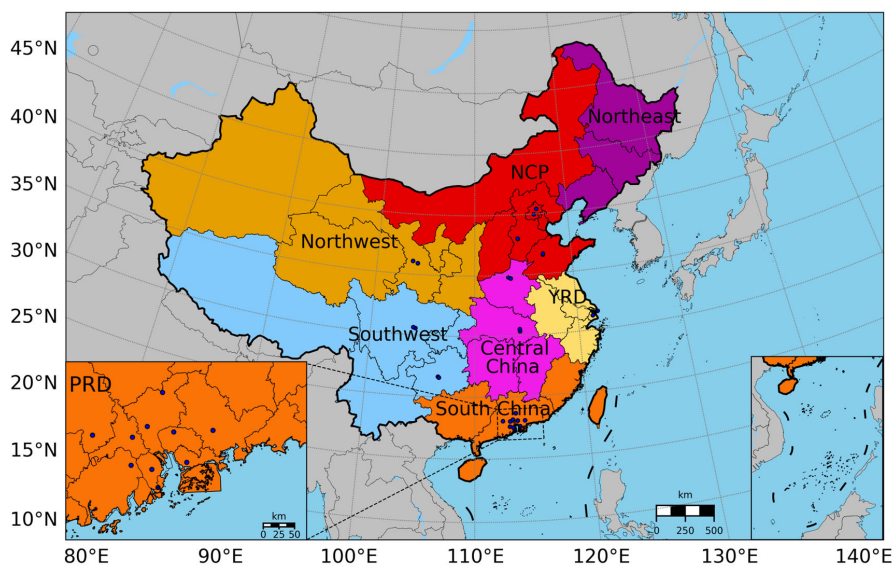
755



756 Table 2. New cases of adjusting emission coefficient under observation constraints

Cases in CMAQ	Changing species in MEIC	Adjusted coefficient
base case	--	--
case_NO _x	NO, NO ₂	1.5
case_ALK2	ALK2	4.6
case_ARO2MN	ARO2MN	3.2
case_BENZ	BENZ	0.4
case_OLE1	OLE1	2.0
case_PRPE	PRPE	2.1
case_ACYE	ACYE	2.8
case_all	all of the above VOCs	

757



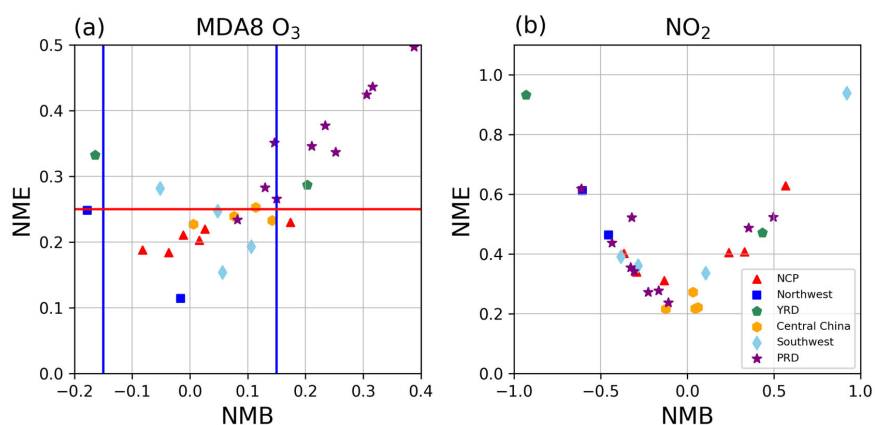
758

759 Figure 1. The CMAQ modelling domain cover China and the surrounding countries and

760 regions in this study, including 28 blue dots that represent the positions of VOCs

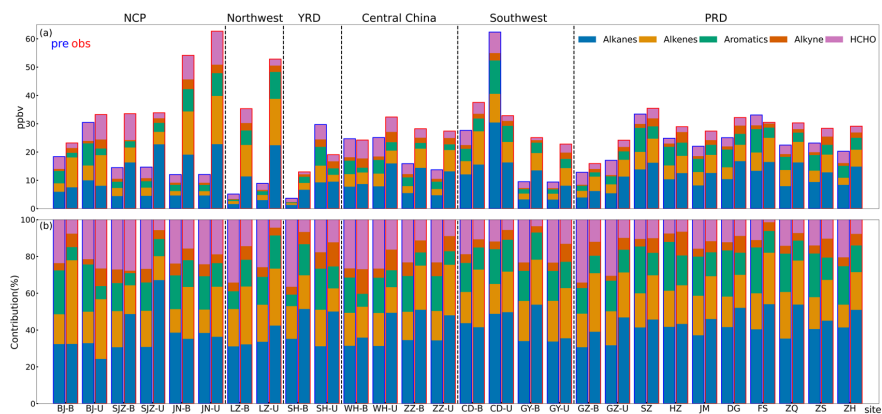


761 sampling sites. We divided China into seven regions according to the geographical
762 location of different provinces, which comprise the following sites: NCP: BJ-B, BJ-U,
763 SJZ-B, SJZ-U, JN-B, JN-U; Northwest: LZ-B, LZ-U; Northeast (No observation site);
764 YRD: SH-B, SH-U; Central China: ZZ-B, ZZ-U, WH-B, WH-U; Southwest: CD-B,
765 CD-U, GY-B, GY-U; South China: Most of the sites are concentrated in PRD region
766 (shown in the enlarged subgraph in the lower left): GZ-B, GZ-U, SZ, HZ, DG, FS, JM,
767 ZQ, ZS, ZH.



768

769 Figure 2. Model performance on MDA8 O₃ and NO₂ of 28 sites in different regions
770 from June 6th to August 24th in 2018. The blue and red lines denote performance
771 criteria for MDA8 O₃ suggested by Emery et al. (2017) and the symbols in different
772 colors distinguish different regions of China.



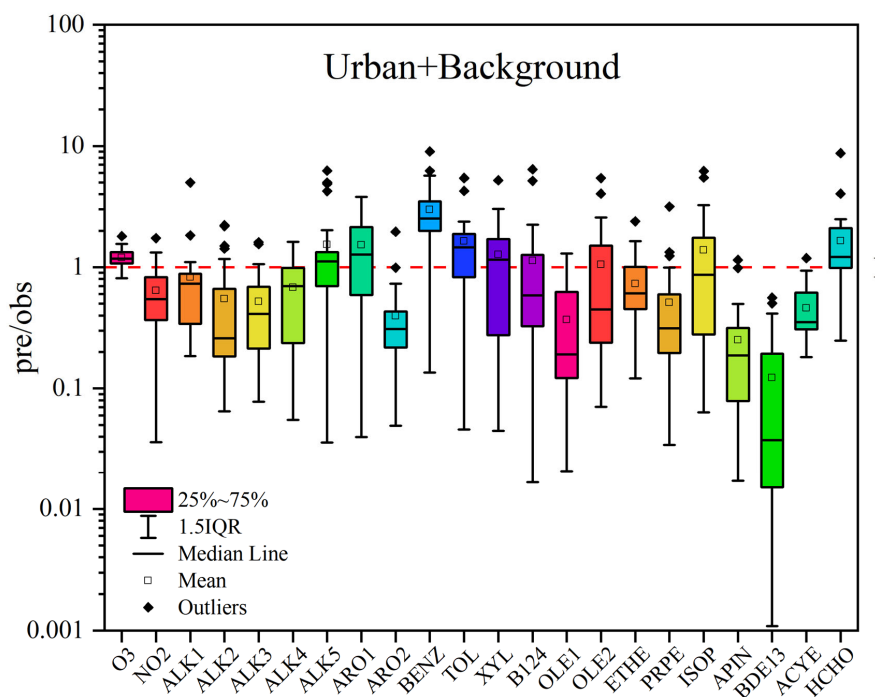
773

774 Figure 3. Comparison of predicted and observed VOCs at 28 sites during the study

775 period. (a) The concentration of VOCs, for each site, on the left are prediction values

776 with a blue edge, and on the right are observation values with a red edge; (b) Percentage

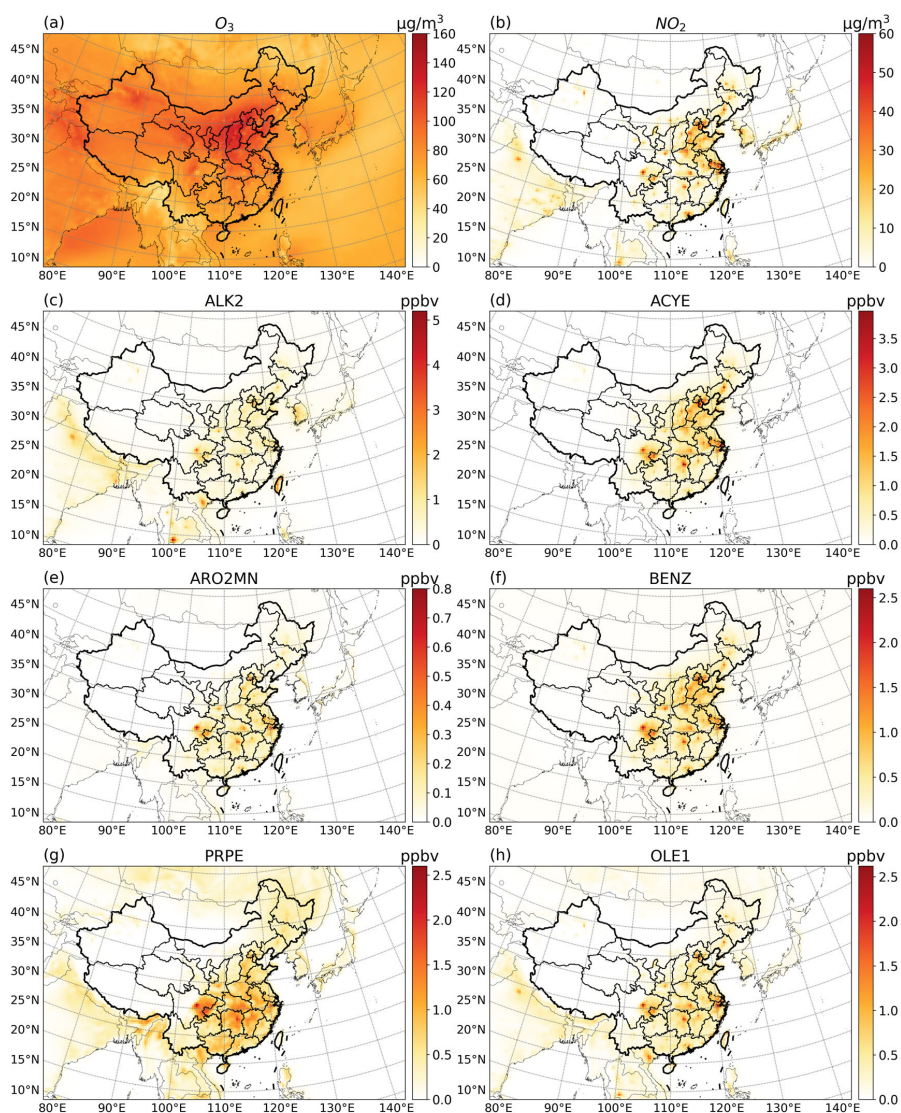
777 of VOCs.



778

779 Figure 4. The predicted/observed ratio (pre/obs) of O₃, NO₂ and different VOCs species
780 at 28 sites (both urban and background). The rectangles with different colors represent
781 the ratio range of 25% to 75% for all sites. The vertical lines with a horizontal bar are
782 called 1.5 Interquartile Range (1.5 IQR). The horizontal lines in rectangles represent
783 the median value and the hollow dots are the mean value. The dots outside the 1.5 IQR
784 are Outliers.

785

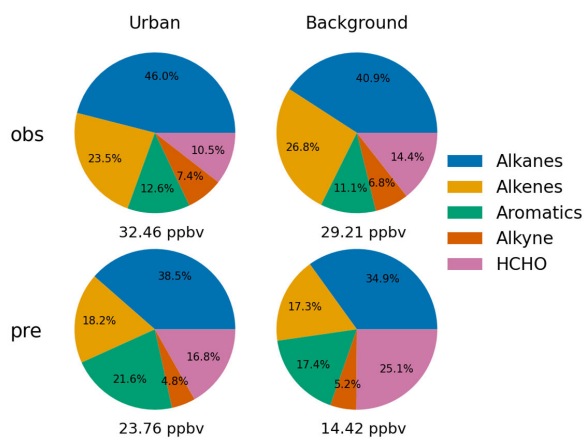


786

787 Figure 5. Prediction concentration of O₃, NO₂ and six VOCs species in the base case

788 from June 6th to August 24th in 2018.

789



790

791 Figure 6. Observed and predicted values of different VOCs species by sites average.